Available online at www.sciencedirect.com
ScienceDirect
Chemical Physics Letters 427 (2006) 432–437
CHEMICAL PHYSICS LETTERS
www.elsevier.com/locate/cplett

Metal-enhanced phosphorescence (MEP)

Yongxia Zhang [a], Kadir Aslan [a], Stuart N. Malyn [a], Chris D. Geddes [a,b,*]

[a] *Institute of Fluorescence, Laboratory for Advanced Medical Plasmonics, Medical Biotechnology Center, University of Maryland Biotechnology Institute, 725 West Lombard Street, Baltimore, MD 21201, USA*
[b] *Center for Fluorescence Spectroscopy, Department of Biochemistry and Molecular Biology, Medical Biotechnology Center, University of Maryland School of Medicine, 725 West Lombard Street, Baltimore, MD 21201, USA*

Received 19 May 2006
Available online 29 June 2006

Abstract

We report the first observation of metal-enhanced phosphorescence (MEP) at low temperature. Silver island films (SiFs) in close proximity to Rose Bengal, significantly enhance the phosphorescence emission intensity. The enhanced phosphorescence intensity is ≈5-fold brighter from SiFs as compared to a glass control sample at 77 K. In addition, enhanced fluorescence emission and spectral narrowing were observed at low temperatures. Our findings suggest that both singlet and triplet states can couple to surface plasmons and enhance both fluorescence and phosphorescence yields. This finding suggests that MEP can be used to promote triplet-based assays, such as those used in photodynamic therapy.

1. Introduction

For clinical applications, the photodynamic property of a lumophore has potential in the diagnosis and treatment of several diseases such as diabetes, peripheral vascular diseases, cerebrovascular and cardiovascular events [1]. Photodynamic therapy is a well-known treatment which can induce cell death when we combine a suitable dye (lumophore), light and oxygen. This effect was observed at least as early as the end of the last century. Raab reported that the dye acridine rapidly killed paramecia when exposed to light, but had no effect in the dark [2]. Light and the lumophore eosin were subsequently combined to treat skin cancer [3].

Over 100 years later, modern photodynamic therapy for the most part is still limited by the insufficient quantity of singlet oxygen, while reacting with biological targets [1,4]. The photodynamic effect includes three primary processes: firstly, the ground state of the dye is optically excited to the excited singlet state, S_n. Then, a population from the excited state is typically transferred to the dye's lowest triplet state by intersystem crossing (a radiationless transition). Finally, collisional energy transfer from the triplet dye to ground-state molecular oxygen ($^3O_2$) produces highly reactive singlet oxygen ($^1O_2$), in turn, returning the dye to its original ground state. The singlet oxygen can react readily with many biological targets and destroy a wide variety of cells [1]. Since singlet oxygen plays a very important role in cell damage, an abundant supply of oxygen is very important. However, if the consumption of oxygen by the photodynamic process is faster than it can be resupplied, it causes oxygen depletion. An alternative method to resolve this problem is to populate high-lying triplet excited states of several dyes which produce oxygen-independent damage [4]. If these excited triplet states obtain sufficient energies to allow for the cleavage of one of the molecular bonds, then radicals that are even more

---

[*] Corresponding author. Address: Institute of Fluorescence, Laboratory for Advanced Medical Plasmonics, Medical Biotechnology Center, University of Maryland Biotechnology Institute, 725 West Lombard Street, Baltimore, MD 21201, USA. Fax: +1 4107064600.
E-mail address: geddes@umbi.umd.edu (C.D. Geddes).

0009-2614/$ - see front matter © 2006 Elsevier B.V. All rights reserved.
doi:10.1016/j.cplett.2006.06.078

reactive than singlet oxygen can be produced. The production of these radicals does not require the presence of oxygen. But both mechanisms i.e. $^1O_2$ and radical, do require high phosphorescence (triplet) quantum yields.

In recent years, our laboratories have both introduced and demonstrated many applications of metal-enhanced fluorescence (MEF) [5–7], metal-enhanced chemiluminescence [8] and indeed plasmon coupled fluorescence [9]. These have included the increased detectability and photostability of fluorophores [5–7,10–12] and chemiluminescent species [8], improved DNA detection [13], the release of self-quenched fluorescence of over labeled proteins [14], enhanced wavelength-ratiometric sensing [15] and the application of metallic surfaces to ultra fast and ultra sensitive target analyte detection [16]. In early interpretations of MEF, we considered the photophysical properties of fluorophores in close proximity to subwavelength size metallic nanostructures were modified by a resonance interaction with the surface plasmons [5–7] (Fig. 1, top), which can be expressed by the following equation:

$$Q_{\mathrm{m}} = (\Gamma + \Gamma_{\mathrm{m}})/(\Gamma + \Gamma_{\mathrm{m}} + k_{\mathrm{nr}}) \quad (1)$$

where Γ is the unmodified radiative decay rate, Γ_{m} is the metal-modified radiative decay rate, k_{nr} are the non-radiative rates and Q_{m} the modified quantum yield. Similarly, the metal modified lifetime Γ_{m} which was thought to be decreased by an increased fluorophore radiative decay rate also could be expressed by the following equation:

$$\tau_{\mathrm{m}} = 1/(\Gamma + \Gamma_{\mathrm{m}} + k_{\mathrm{nr}}) \quad (2)$$

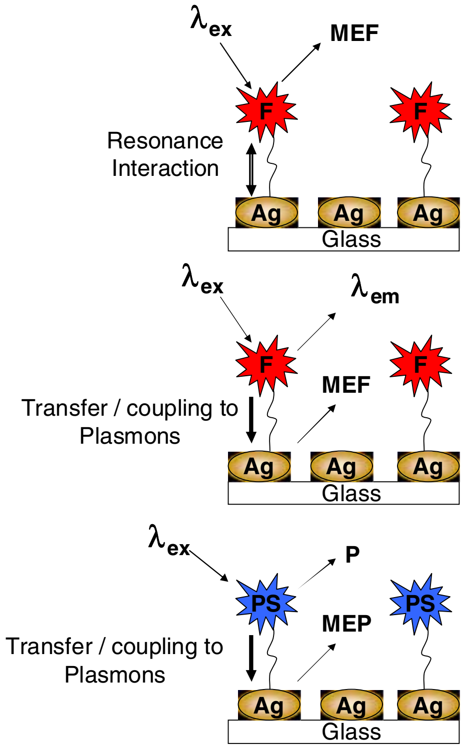

Fig. 1. Graphical representation of metal-enhanced fluorescence (top and middle), and for metal-enhanced phosphorescence (bottom). F – fluorophore, RB – Rose Bengal, P – phosphorescence and MEP – metal-enhanced phosphorescence.

These equations have been widely used in our laboratories to explain the MEF phenomenon which was observed for fluorophore-metal combinations: increasing quantum yields and reduced fluorophore lifetimes when in close proximity to metallic nanostructures [5–7]. However, recently our interpretation of MEF has shifted somewhat to a model whereby non-radiative energy transfer occurs from excited distal fluorophores to the surface plasmon electrons in *non-continuous* films (Fig. 1 middle). The surface plasmons in turn, radiate the photophysical characteristics of the coupling fluorophores [17]. This explanation has been facilitated by our recent finding of surface plasmon coupled emission (SPCE) [19], whereby fluorophores distal to a *continuous* metallic film can directionally radiate fluorophore emission at a unique angle from the back of the film. Remarkably, the plasmon coupled emission is completely p-polarized, irrespective of the excitation polarization [9,18]. Similarly, it also has been hypothesized that MEF is plasmon coupled but not so highly directional, as is the case with SPCE [19], the scattering properties of the particulate nanostructures playing a very important role in plasmon emission coupling, where larger silver nanostructures have been shown experimentally to be more efficient at coupling and radiating fluorescence than small ones [20]. In this regard, the extinction properties of metal particles can be expressed by a combination of absorption (C_{A}) and scattering (C_{S}) factors. In the Mie limit [20]

$$C_{\mathrm{E}} = C_{\mathrm{A}} + C_{\mathrm{S}} = k_1\,\mathrm{Im}(\alpha) + \frac{k_1^4}{6\pi}|\alpha|^2 \quad (3)$$

where $k_1 = 2\pi n_1/\lambda_0$ is the wavevector of the incident light in medium I and α is the polarizability of the sphere with radius r, n_1 is the refractive index and λ_0 the incident wavelength. The term $|\alpha|^2$ is square of the modulus of α [20].

$$\alpha = 4\pi r^3(\varepsilon_m - \varepsilon_1)/(\varepsilon_m + 2\varepsilon_1) \quad (4)$$

where ε_1 and ε_m are the dielectric and the complex dielectric constants of the metal, respectively.

The current interpretation of MEF [20] is therefore one underpinned by the scattering component of the metal extinction which is shown in the second term of Eq. (3). Since larger particles have wavelength distinctive scattering spectra (C_{S}) as compared to their absorption spectra (C_{A}), then plasmon coupled emission (MEF) from larger nanoparticles is more efficient [20].

Subsequently, in this Letter we show that mental-enhanced phosphorescence (MEP) is also surface plasmon coupled as shown in Fig. 1, bottom, where non-radiative energy transfer occurs from excited distal lumophores to the surface plasmon electrons in non-continuous silver films, which in turn radiate Rose Bengal emission efficiently. The phosphorescence intensity is observed ≈5-fold brighter from SiFs as compare to glass, a control sample also at 77 K. This observation is not only helpful in our understanding of plasmon–lumophore interactions, but suggests that this approach may be of significance for phosphorescence triplet state based clinical assays such as those used in photodynamic therapy, where high triplet yields are preferred [4]. In this Letter, we report our MEP findings using Rose Bengal (RB), a dye that has been found to produce oxygen independent cell damage and excited triplet states producing higher reactive radicals [21].

2. Experimental

2.1. Materials

Silver nitrate (99.9%), sodium hydroxide (99.996%), ammonium hydroxide (30%), D-glucose and premium quality Silane-prep™ glass slides (75 × 25 mm), ethanol (HPLC/spectrophotometric grade) were obtained from Sigma-Aldrich. All chemicals were used as received.

2.2. Methods

Silver island films (SiFs) were prepared as we have previously published [7]. In a typical SiFs preparation, a solution of silver nitrate (0.5 g in 60 ml of deionized water) is placed in a clean 100-ml glass beaker. 200 μl of freshly prepared 5% (w/v) sodium hydroxide solution and 2 ml of ammonium is added to a continuously stirred silver nitrate solution at room temperature. Subsequently, the solution is cooled to 5 °C by placing the beaker in an ice bath, followed by soaking the Silane-prep™ glass slides in the solution and adding a fresh solution of D-glucose (0.72 g in 15 ml of water). Then, the temperature of the mixture is allowed to warm to 30 °C. As the color of the mixture turned from yellow green to yellowish brown, the slides are removed from the mixture, washed with water, and sonicated for 1 min at room temperature.

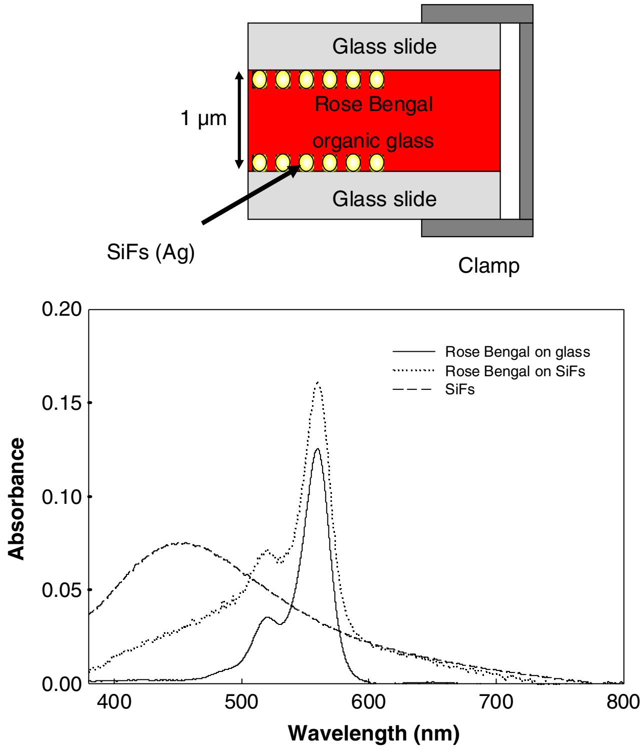

Fig. 2. Sandwich experimental geometry (top). Absorption spectra at room temperature of SiFs and Rose Bengal immobilized in an organic glass, sandwiched between two silvered and unsilvered slides, respectively (bottom).

300 μl of Rose Bengal (1.0×10^{-4} M) in ethanol solution was dropped in a sandwich format between the glass slides and the silver island films, respectively. Fig. 2, top, shows the experimental sample geometry. The glass/SiFs surfaces were immersed in liquid nitrogen for 2 min and used for low temperature (77 K) measurements. Absorbance spectra were performed using a Varian Cary 50 UV–Vis spectrophotometer. Fluorescence and phosphorescence measurements were performed at 45° to the excitation through a long pass filter, using a Fiber Optic Spectrometer (HD2000), Ocean Optics, Inc.

3. Results

Fig. 2, bottom, shows the absorption spectra of SiFs and Rose Bengal from between the SiFs and from the glass. At low temperatures the SiF plasmon absorption spectra did

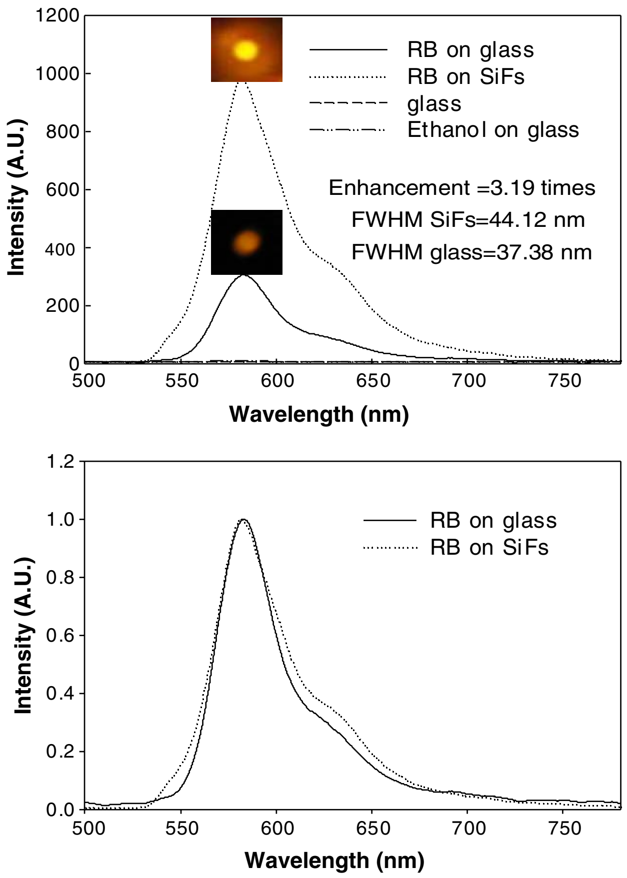

Fig. 3. Fluorescence emission spectra, Ex = 532 nm, of Rose Bengal sandwiched between two silvered and unsilvered slides at room temperature, (top), and the normalized emission spectra from both glass and silver (bottom). RB – Rose Bengal.

not change from that observed at room temperature. Uncoated SiFs and glass were used as reference backgrounds for the Rose Bengal absorption measurements, respectively. From Fig. 2, bottom, it can be seen that the Rose Bengal has much larger absorbance on SiFs as compared to glass. These effects can be explained as a result of the coupling of the fluorophore/lumophore dipole with the localized electromagnetic field of the metallic particles, efficiently increasing the absorption cross-section of the lumophore [7]. It is well-known that conducting metallic particles can modify the free space absorption condition in ways that increase the incident electric field, E_m, felt by Rose Bengal, effectively increasing the excitation rate of the fluorophore [22]. The enhanced absorption of dye molecules near metallic surfaces was firstly reported by Glass et al., in 1980 and also confirmed by other groups [23–25]. In addition, the enhanced absorption can lead to surface enhanced luminescence phenomenon, such as MEF [5–7]. The absorption spectra of Rose Bengal from between the SiFs show significant broadening as compared to that on glass, strongly suggesting enhanced Rose Bengal optical absorption.

Fig. 3, top, shows the fluorescence emission spectra of Rose Bengal on SiFs and glass at room temperature. The enhanced fluorescence intensity was >3-fold brighter from the silver, as compared to glass, where both spectra are identical when normalized (Fig. 3, bottom). Previous studies of the MEF phenomenon have reported a reproducible enhancement of between 2- and 10-fold using simple SiFs [26]. In this regard it should be noted that the *true* metal-enhanced fluorescence enhancement factor is much larger here than 3, and is ≈75-fold. This is because the MEF phenomenon is through-space with an interaction distance of less than 20 nm. With a sample thickness of 1 μm, Fig. 2 top, then only 4% of the sample is within the MEF enhancement region, hence the true enhancement factor is approximately 25 times larger. Fig. 3, top, photograph also shows that the emission intensity is much more clearly detectable from between SiFs than from the glass control slide. In addition to close proximity nanostructures, there are also several other factors that can influence the magnitude of the MEF phenomenon, such as temperature. It can be expected that if all other factors remain constant, the quantum efficiency of fluorescence will decrease with

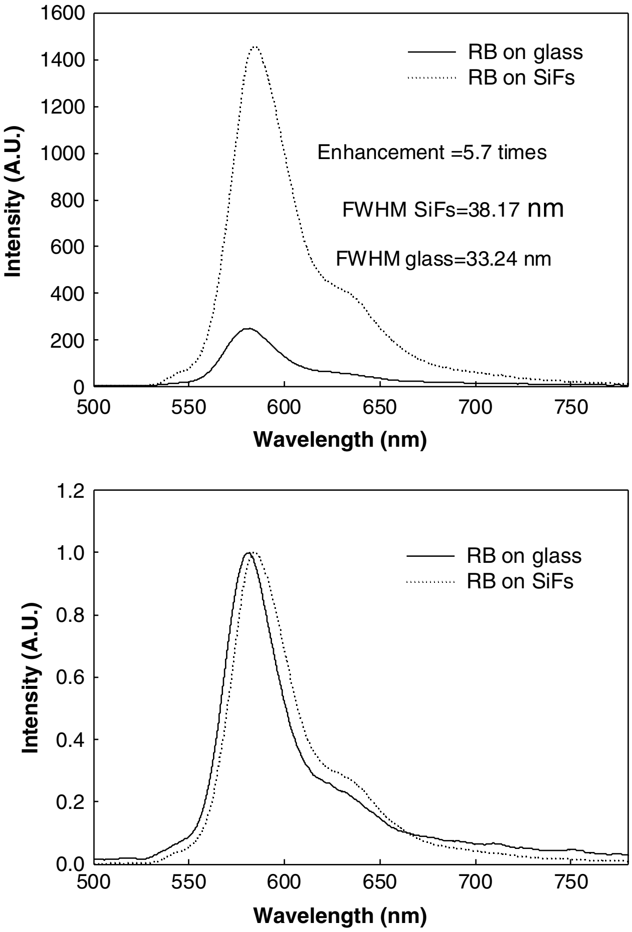

Fig. 4. Fluorescence emission spectra of Rose Bengal at 77 K between both silvered and unsilvered glass slides (top), and the normalized emission spectra (bottom). $\lambda_{ex} = 532$ nm. RB – Rose Bengal.

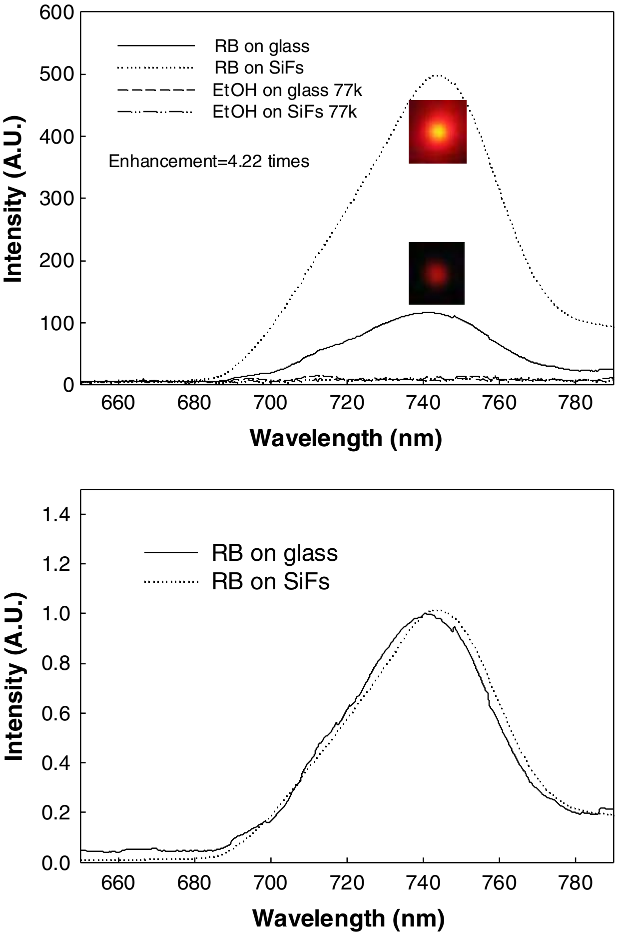

Fig. 5. Phosphorescence spectra of Rose Bengal immobilized in an organic glass from between both silvered and unsilvered glass slides at 77 K (top) and the normalized phosphorescence emission spectra (bottom). $\lambda_{ex} = 532$ nm.

increasing temperature [27]. Fig. 4 shows the fluorescence emission spectra of Rose Bengal from between the SiFs and from glass at 77 K. It can be seen that the enhanced fluorescence intensity was >5-fold brighter from silver as compared to glass and the full width at half maximum (FWHM) of fluorescence emission spectra was ≈38 nm which is narrower as compared that measured at room temperature, *cf.* 44 nm. However, the shape of the fluorescence emission spectra at 77 K is identical to that of the spectra measured at room temperature.

Metal-enhanced phosphorescence (MEP) of Rose Bengal on SiFs was studied, Fig. 5, also at low temperature. Phosphorescence is not readily observed at room temperature because of collisional deactivation and the presence of quenching impurities. Phosphorescence signals can however be observed at low temperatures and in media where the diffusion of both the lumophores and oxygen is negligible, such as in organic glasses as reported here. From Fig. 5, the enhanced phosphorescence intensity was >5-fold brighter from the silver, as compare to glass (Fig. 5, top) and both spectra are identical when normalized (Fig. 5, bottom). The photograph inset of Fig. 5 also shows the enhanced phosphorescence visibly from both glass and SiFs. The emission intensity is clearly detectable from between the SiFs, but much weaker from the glass control slide. To the best of our knowledge, this is the first observation of metal-enhanced phosphorescence (MEP).

4. Discussion

At first consideration one may be surprised by the presence of both enhanced MEP and MEF as both processes are competitive, both providing for deactivation of electronic excited states. As described in the introduction, and indeed shown in Fig. 1 middle, MEF is currently thought to occur due to the efficient non-radiative transfer to surface plasmons, which themselves efficiently radiate the photophysical characteristics of the fluorophore [20]. For MEP, a similar process is also thought to occur as depicted by Fig. 1, bottom. Similarly, our group has also recently shown that chemiluminescence species, which are electronically excited as the result of a chemical reaction, can also be plasmon enhanced by the presence of silver nanostructures, namely Metal-enhanced chemiluminescence (MEC) [8]. At present we have two possible explanations for the occurrence of both MEF and MEP in the same system. Firstly, we have observed enhanced Rose Bengal absorption from between SiFs, Fig. 2, bottom. It therefore seems reasonable that a net system absorption would facilitate both MEP and MEF simultaneously, as we have observed, Figs. 3–5. Alternatively, Rose Bengal is known to undergo reverse intersystem crossing or sometimes called back intersystem crossing, which is the inverse of the more-common S_1–T_1 intersystem crossing, where S_1 and T_1 are lowest singlet and triplet states, respectively [27]. For enhanced direct triplet absorption, the MEF and MEP processes for Rose Bengal may not be competing but more likely are complimentary processes, especially if the singlet and triplet energy levels are similar. In this case, it seems reasonable that both states, S_1 and T_1, could both induce and couple to surface plasmons as has been observed many times by our laboratory for enhanced S_1 emission at room temperature [5–7].

5. Conclusions

In this Letter, we have shown the first observation of low-temperature metal-enhanced phosphorescence. Rose Bengal in close proximity to silver island films can produce enhanced phosphorescence, a 5-fold increase was observed as compared to an identical control sample containing no silver. Metal-enhanced phosphorescence (MEP) may be of significance for phosphorescence based clinical assays such as those used in photodynamic therapy. In addition, this finding suggests that photon induced electronic excited states at low temperature can both induce and couple to surface plasmons facilitating both enhanced fluorescence, S_1, and phosphorescence, T_1, emission. The degree of enhanced triplet yields (triplet quantum yields) and the subsequent rates of singlet oxygen production of lumophores/fluorophores in close proximity to plasmonic structures, for potential downstream applications in photodynamic therapy, will be reported by us in due course.

Acknowledgements

The authors would like to thank University of Maryland Biotechnology Institute for salary support.

References

[1] T.J. Dougherty et al., J. Natl. Cancer Inst. 90 (1998) 889.
[2] O. Raab, Infusoria Z. Biol. 39 (1900) 524.
[3] V.H. Tappeiner, A. Jesionek, Muench. Med. Wochneshr. 47 (1903) 2042.
[4] H.I. Pass, J. Natl. Cancer Inst. 85 (1993) 443.
[5] K. Aslan, I. Gryczynski, J. Malicka, E. Matveeva, J.R. Lakowicz, C.D. Geddes, Curr. Opin. Biotechnol. 16 (1) (2005) 55.
[6] C.D. Geddes, K. Aslan, I. Gryczynski, J. Malicka, J.R. Lakowicz, Noble metal nanostructure for metal-enhanced fluorescence, in: Review Chapter for Annual Reviews in Fluorescence, Kluwer Academic/Plenum Publishers, NY, USA, 2004, p. 365.
[7] C.D. Geddes, K. Aslan, I. Gryczynski, J. Malicka, J.R. Lakowicz, Radiative decay engineering, in: Topics in Fluorescence in Fluorescence Spectroscopy, Kluwer Academic/Plenum Publishers, NY, USA, 2005, p. 405.
[8] M.H. Chowdhury, K. Aslan, J.R. Lakowicz, C.D. Geddes, Appl. Phys. Lett. 88 (2006) 173104.
[9] J.R. Lakowicz, Anal. Biochem. 324 (2) (2004) 153.
[10] J.R. Lakowicz, Anal. Biochem. 298 (2001) 1.
[11] J.R. Lakowicz, Y. Shen, S. D'Auria, J. Malicka, J. Fang, Z. Grcyzynski, I. Gryczynski, Anal. Biochem. 301 (2001) 261.
[12] J.R. Lakowicz, Y. Shen, Z. Grcyzynski, S. D'Auria, I. Gryczynski, Biochem. Biophys. Res. Commun. 286 (2001) 875.
[13] J. Malicka, I. Gryczynski, J.R. Lakowicz, Biochem. Biophys. Res. Commun. 306 (2003) 213.
[14] J.R. Lakowicz, J. Malicka, S. D'Auria, I. Gryczynski, Anal. Biochem. 320 (2003) 13.

[15] K. Aslan, J.R. Lakowicz, H. Szmacinski, C.D. Geddes, J. Fluoresc. 15 (1) (2005) 37.
[16] K. Aslan, C.D. Geddes, Anal. Chem. 77 (24) (2005) 8057.
[17] J.R. Lakowicz, Anal. Biochem. 337 (2) (2005) 171.
[18] I. Gryczynski, J. Malicka, Z. Gryczynski, J.R. Lakowicz, Anal. Biochem. 324 (2) (2004) 170.
[19] C.D. Geddes, I. Gryczynski, J. Malicka, J.R. Lakowicz, Photon. Spectra (2004).
[20] K. Aslan, Z. Leonenko, J.R. Lakowicz, C.D. Geddes, J. Fluoresc. 15 (2005) 643.
[21] M.A.J. Rodgers, Chem. Phys. Lett. 78 (1981) 509.
[22] C.D. Geddes, J.R. Lakowicz, J. Fluoresc. 12 (2002) 121.
[23] A.M. Glass, P.F. Liao, J.G. Bergman, D.H. Olson, Opt. Lett. 5 (1980) 368.
[24] H.G. Craighead, A.M. Glass, Opt. Lett. 6 (1981) 248.
[25] S. Garoff, D.A. Weitz, T.J. Gramila, C.D. Hanson, Opt. Lett. 6 (1981) 245.
[26] K. Aslan, J.R. Lakowicz, C.D. Geddes, Anal. Bioanal. Chem. 382 (2005) 926.
[27] J.R. Lakowicz, Principles of Fluorescence Spectroscopy, Kluwer Academic/Plenum Publishers, NY, USA, 1999.